Structural Details of Asp(B9) Human Insulin at Low pH from Two-Dimensional NMR Titration Studies†

Morten Dahl Sørensen and Jens J. Led*

Department of Chemistry, University of Copenhagen, The H. C. Ørsted Institute, Universitetsparken 5, DK-2100 Copenhagen Ø, Denmark

Received June 23, 1994; Revised Manuscript Received August 29, 1994®

ABSTRACT: A titration study of the dimeric Asp(B9) mutant of human insulin was performed using two-dimensional NMR spectroscopy. Based on 10 NOESY spectra recorded in the pH range 1.73−3.93, the pK_a values of the seven carboxyl groups in the mutant were determined, and the titration shifts of 46 pH-dependent protons in non-ionizable groups were investigated. Further, the pK_a values of the two histidine imidazole rings were determined from a series of 1D spectra recorded in the pH range 6.65−10.0. The titration shifts of all pH-dependent protons were analyzed by a nonlinear least-squares fitting procedure, using an equation that describes a one-step titration. Also the pH dependence of the exchange rate of the amide proton of Phe(B24) was determined in the applied pH range. On the basis of the experimental results, it is concluded that the Asp(B9) residue forms an N-cap of the B-chain α-helix through an interaction between the side-chain carboxyl group of the residue and the dipole of the helix. Further, the titration data show that salt bridges are established between Glu(B13) and His(B10) and between Asn(A21) and Arg(B22) at pH values, where the interacting groups are ionized, and that a hydrogen bond exists between the amide proton of Val(A3) and the C-terminal carboxyl group of Thr(B30). Most surprisingly, the data analysis shows that the Asp(B9) insulin exists as a dimer throughout the investigated pH range, that is, also at pH values where there is a substantial negative charge repulsion in the monomer−monomer interface of the dimer.

The increasing number of NMR[1] solution structures of small proteins that are being presently determined provides a valuable basis for further studies of the molecular characteristics of the proteins, such as folding, structural changes, aggregation, dynamics, and function. Moreover, the same multi-dimensional NMR techniques that have impelled this development also provide the tools for studying these molecular characteristics. Thus, when the sequential assignments of the NMR spectra have been made and the structure has been determined, the atomic level resolution of the NMR spectra allows a determination of the molecular characteristics in detail and to a degree unsurpassed by any other techniques.

Here we present a detailed two-dimensional (2D) NMR study of a series of molecular properties of the Asp(B9) mutant of human insulin (Figure 1). The three-dimensional NMR solution structure of this mutant was determined previously (Jørgensen et al., 1992), and it was found that the mutant forms a regular dimer at the applied pH of 1.9. In the present study, we have investigated a series of electrostatic interactions, hydrogen bonds, and structural changes of the mutant through their dependence on pH. In particular, we have investigated the dimer → monomer transition with increasing pH.

MATERIALS AND METHODS

Human Asp(B9) insulin was made by specific alteration of the amino acid sequence at the ninth position in the B-chain (Ser → Asp) through DNA technology (Brange et al., 1988). After purification by reverse-phase HPLC, the purity of the insulin was at least 98%.

The samples used in the titration experiments were prepared by suspension of 11.4 mg of lyophilized Asp(B9) insulin in 1 mL of H_2O/D_2O (90%/10%, v/v). The protein was dissolved by adjusting the pH to 2.8. The final concentration of Asp(B9) insulin was 1.7 mM. Similarly, three 4.7 mM insulin samples in D_2O were prepared: one for the titration of the imidazole rings in His(B5) and His(B10) and two for the determination of the exchange rate of the Phe(B24) amide proton with deuterium. The latter were prepared less than 20 min before the start of the data acquisition. The pH was adjusted with dilute HCl and NaOH (or in the case of samples in D_2O with DCl and NaOD) and determined at 22 °C using a Radiometer PHM80 meter equipped with a 3-mm glass electrode. All values refer to direct meter readings. The pH was measured before and after the data acquisition. The two values agreed within 0.1 unit. The average of the two values was used in the fitting process. In all cases, dioxane was added as an internal reference, and the proton chemical shifts were measured relative to dioxane at 3.75 ppm. The spectra were recorded on 550-μL samples in 5-mm NMR tubes.

† This work was supported by the Danish Technical Research Council, J. Nos. 16-4679.H, 16-5027, and 16-5028; the Danish Natural Science Research Council, J. No. 11-8977-1; the Ministry of Industry, J. No. 85886; Julie Damms Studiefond, and Direktør Ib Henriksens Fond.

* Author to whom all correspondence should be addressed.

® Abstract published in *Advance ACS Abstracts,* October 15, 1994.

[1] Abbreviations: BPTI, bovine pancreatic trypsin inhibitor; FID, free induction decay; HPLC, high-performance liquid chromatography; NMR, nuclear magnetic resonance; NOE, nuclear Overhauser enhancement; NOESY, NOE correlated spectroscopy; 2D, two-dimensional; ppm, parts per million; TMS, tetramethylsilane; TPPI, time proportional phase increment.

0006-2960/94/0433-13727$04.50/0

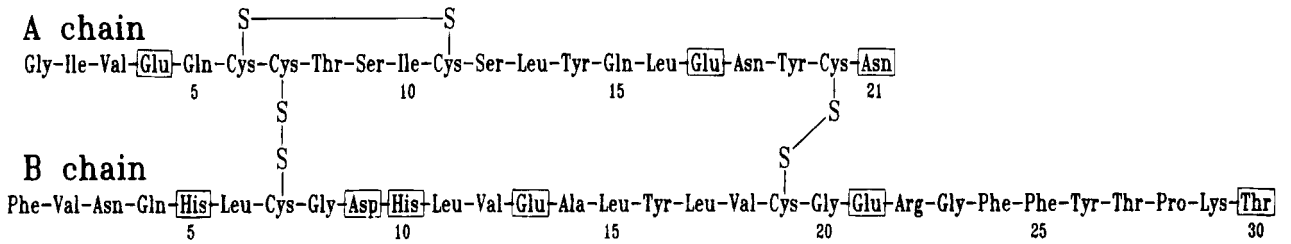

FIGURE 1: Amino acid sequence of Asp(B9) insulin. The seven residues with carboxyl groups and the two histidines are boxed.

The NMR experiments were performed at 295 K on a Bruker AM500 NMR spectrometer equipped with an Aspect 3000 computer. The titration data were obtained from a series of 2D NOESY spectra (Jeener et al., 1979; Macura et al., 1981) recorded at pH 1.73, 1.93, 2.20, 2.52, 2.85, 3.02, 3.25, 3.46, 3.73, and 3.93, respectively. The mixing time was 160 ms in all cases. Each of the 10 2D FIDs consisted of 2048 data points in the t_2 dimension and 800 data points in the t_1 dimension. A total of 64 scans was accumulated for each t_1 increment. The spectra were recorded with sequential quadrature in the t_2 dimension (Redfield & Kunz, 1975) and with time proportional phase increment (TPPI) in the t_1 dimension (Drobny et al., 1979; Bodenhausen et al., 1980; Marion & Wüthrich, 1983). The spectral width was 7463 Hz in both dimensions. The water signal was partially suppressed by phase-coherent, continuous irradiation during the preparation period (1 s) and the mixing period (Hurlt, 1976; Zuiderweg et al., 1986). The residual water signal was attenuated by convolution of the time−domain data, using a 90° shifted sine bell convolution weighting function (Marion et al., 1989). Subsequently, the data were multiplied in the t_2 dimension by a squared sine bell function shifted 90° and a sine bell function shifted 70° and in the t_1 dimension by a squared sine bell function shifted 90° and a sine bell function shifted 60°. Finally, before Fourier transformation, the FID was zero-filled to 4096 data points in the t_2 dimension and to 2048 data points in the t_1 dimension.

The 1D ^{1}H spectra used for the determination of pK_a values of the two imidazole rings in His(B5) and His(B10) were recorded at pD 6.65, 6.96, 7.26, 7.55, 7.96, 8.27, 8.62, 9.00, 9.31, 9.60, and 10.0, respectively. The individual spectra were sums of 128 accumulations and consisted of 16384 data points. The spectral width was 10 000 Hz.

Finally, the series of 1D ^{1}H spectra used to determine the exchange rate of the Phe(B24) amide proton were recorded at pH 1.92 and 3.03, respectively. At pH 1.92, a total of 44 spectra were recorded over a period of 13 h, while 41 spectra were recorded at pH 3.03 over a period of 17.4 h. The spectra in the two series were the sum of 64 and 128 accumulations and consisted of 32 768 and 16 384 data points, respectively. The spectral width was 10 000 Hz in both series.

The pH dependences of the proton chemical shifts were analyzed by a nonlinear least-squares fit using the equation that describes a one-step titration:

$$\delta_{obs} = \delta_1 x + (1 - x)\delta_2 \quad (1)$$

Here δ_{obs} is the observed chemical shift, while δ_1 and δ_2 are the chemical shifts of the species in which the ionizable group is protonated or deprotonated, respectively. The molar fraction of the protonated form, x, is given by

$$x = 1 - \frac{1}{1 + 10^{pK_{app} - pH}} \quad (2)$$

where K_{app} is the apparent ionization constant of the ionizable group. In most cases, the observed chemical shifts were obtained as an average of values measured from two or more intraresidual cross peaks.

In order to obtain the highest possible precision, the pK_a values of the individual carboxyl groups and imidazole groups were determined by a *simultaneous* fit of the parameters in eq 1 to the chemical shifts of the adjacent, intraresidual protons given in Table 1. In the analysis, these chemical shifts were assumed not to be affected by other ionizable groups. The result of the simultaneous fit used to determine the pK_a value of Thr(B30) is shown in Figure 2.

The exchange rates of the Phe(B24) amide proton with deuterium were determined by a least-squares fit of the intensity of the Phe(B24) NH resonance to a single-exponential function:

$$I(t) = I_0 e^{-kt} \quad (3)$$

where $I(t)$ is the intensity at time t, I_0 the initial intensity, and k is the exchange rate. The intensities were obtained from the spectra by a nonlinear least-squares fit of the expression for the discrete Fourier transformation to the experimental data (Abildgaard et al., 1988).

RESULTS

Figure 3 shows the fingerprint region of two NOESY spectra recorded at pH 1.73 and pH 3.47, respectively. The assignments of intraresidual NH−H$^\alpha$ cross peaks at pH 1.73 are based on the sequence-specific ^{1}H assignments at pH 1.85 (Kristensen et al., 1991), while the assignment at pH 3.47 was obtained by tracing the cross peaks through the series of pH-dependent 2D NOESY spectra. As it appears from Figure 3, some of the signals move significantly with changes in pH (e.g., A3, A4, and B9), while others are almost unaffected (e.g., A13 and B21).

The obtained pK_a values for the nine ionizable groups are listed in Table 1. The pK_a values obtained for the seven carboxyl groups fall in a wide range, implying that some of them take part in salt bridges and/or hydrogen bonds. Individual assignments of the pK_a values of the imidazole rings of the two histidines, B5 and B10, could not be obtained on the basis of the sequence-specific ^{1}H assignment of Asp(B9) insulin, since this assignment is unknown above the isoelectric point.

The titration shifts of 196 protons in the non-ionizable groups of the insulin mutant were measured. Figure 4 illustrates the titration of three of the protons in Asp(B9) insulin. Between pH 1.73 and pH 3.93, a total of 73 proton

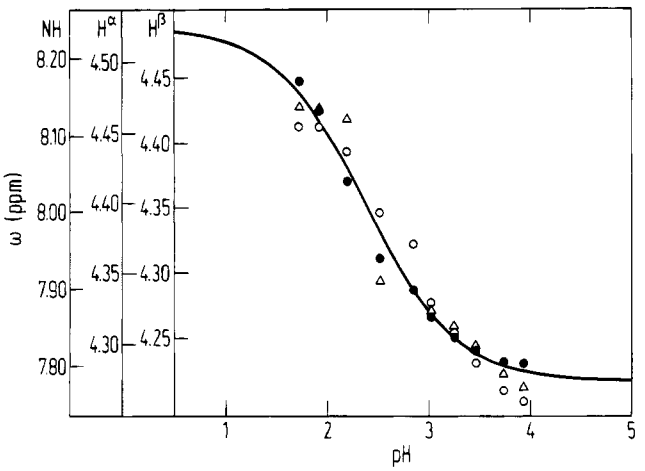

FIGURE 2: Result of a simultaneous fit of the parameters in eq 1 to the chemical shifts of NH (●), H^α (△), and H^β (○) protons of Thr(B30). The obtained pK_a value of Thr(B30) is listed in Table 1.

Table 1: Ionization Constants[a] of Nine Ionizable Groups in B9(Asp) Insulin at 295 K

residue	group	pK_a	protons[b]	pK_{int}[c]
Glu(A4)	γ-COOH	2.62 ± 0.06	NH, H^α, H^γ	4.5
Glu(A17)[d]	γ-COOH	>3.7		4.5
Asn(A21)	α-COOH	3.17 ± 0.04	NH, $H^{\beta'}$, H^δ, $H^{\delta'}$	3.6
Asp(B9)	β-COOH	2.60 ± 0.05	NH, H^α, H^β, $H^{\beta'}$	4.0
Glu(B13)	γ-COOH	2.20 ± 0.10	H^γ, $H^{\gamma'}$	4.5
Glu(B21)	γ-COOH	3.71 ± 0.04	H^γ	4.5
Thr(B30)	α-COOH	2.38 ± 0.08	NH, H^α, H^β	3.6
His I	imidazole	6.915 ± 0.068	C2H	6.8
His II	imidazole	7.040 ± 0.036	C2H	6.8

[a] The pK_a values of the carboxyl groups are determined in H_2O while the pK_a values of the two imidazole rings are determined in D_2O. [b] Protons used in the fitting procedure; see text. [c] Intrinsic pK_a value, that is, the value in the absence of any influence from other charged sites on the protein, from States and Karplus (1987). [d] None of the protons in this residue had any significant titration shift, implying that the pK_a value is outside the experimental pH range.

resonances show chemical shift variations larger than 0.03 ppm. As a first approximation, these resonances were taken to be pH-dependent, and their chemical shift variations were analyzed using eq 1. Proton resonances affected by more than one ionizable group are likely to give calculated parameters ($\Delta\delta = \delta_2 - \delta_1$, pK_{app}) with large standard deviations (Kohda et al., 1991; Abildgaard et al., 1992). Therefore, only proton resonances with standard deviations of the pK_{app} values less than 10% were considered here, which results in a total of 46 pH-dependent protons in non-ionizable groups. The pK_{app} values of these protons are given in Table 2.

The results of the experiments in which the exchange rate of the Phe(B24) amide hydrogen was determined are shown in Figure 5. The obtained exchange rates were (43.3 ± 0.5) × 10^{-6} s^{-1} and (40.1 ± 0.6) × 10^{-6} s^{-1} at 295 K and pH 1.92 and 3.03, respectively.

DISCUSSION

Interaction between Asp(B9) and the Dipole of B-Chain α-Helix. The high frequency with which negatively and positively charged residues are observed near the N- and C-terminals of helices, respectively, can be rationalized by the formation of favorable interactions between the charged residue and the α-helix dipole, which is positive at the

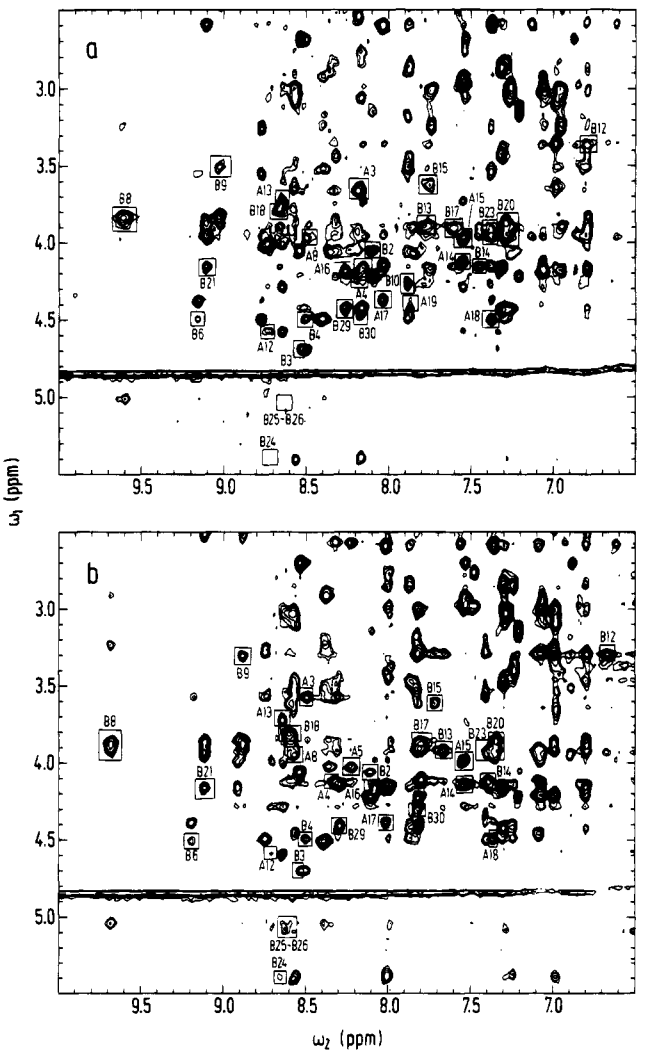

FIGURE 3: NOESY spectra of Asp(B9) insulin in H_2O (1.7 mM, 295 K) recorded at (a) pH 1.73 and (b) pH 3.47. The region shown contains correlations between amide and α-protons. Assigned intraresidual NH−H^α cross peaks are labeled. The labels B24 and B25−B26 in panel a correspond to cross peaks observed in a NOESY spectrum recorded at pH 1.90, 295 K, and 5 mM [Figure 3 of Kristensen et al. (1991)].

N-terminal and negative at the C-terminal (Šali et al., 1988; Nicholson et al., 1988). A favorable interaction between the α-helix dipole and the charged residue results in a lowering of the pK_a value when the residue is negatively charged and in a raising when the residue is positively charged.

Asp(B9) insulin has an α-helix in the B-chain extending from Gly(B8) to Cys(B19) (Kristensen et al., 1991; Jørgensen et al., 1992). Therefore, the pK_a value of Asp(B9) is expected to be lower than the intrinsic pK value, pK_{int}, which is the pK_a value of the ionizable group in the absence of any electrostatic interactions. For Asp, pK_{int} = 4.0 (States & Karplus, 1987) while a pK_a of 2.60 ± 0.05 is observed for Asp(B9) in the insulin mutant here (Table 1). Immediately, this difference in the pK_a value suggests a charge−dipole interaction, although hydrogen bonds or salt bridges could, in principle, also give rise to the observed lowering of the pK_a value. However, the latter two possibilities are less likely here, as shown in the following.

The hydrogen bond can be ruled out on the basis of the refined solution NMR structure of Asp(B9) insulin at pH 1.9 (Jørgensen et al., 1992), since this structure shows no

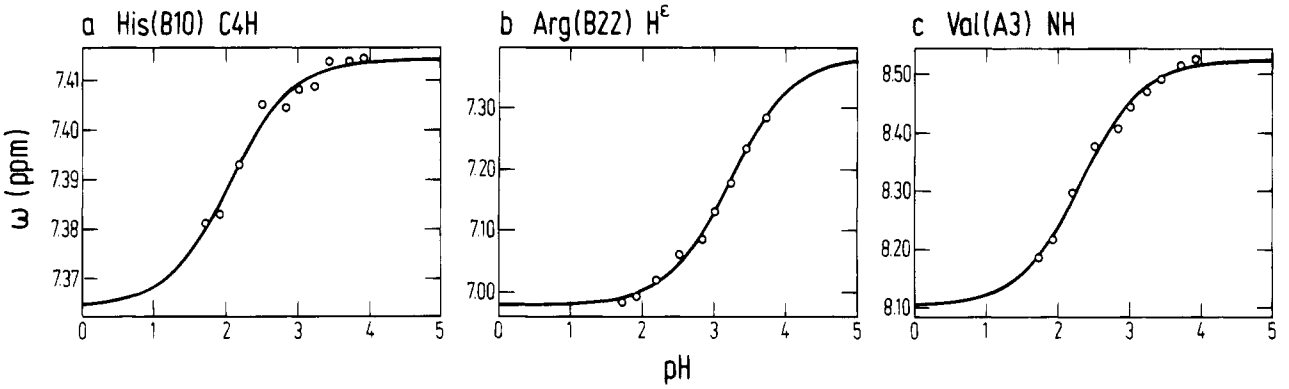

FIGURE 4: Dependence on pH of (a) His(B10) C4H, (b) Arg(B22) H^{ϵ}, and (c) Val(A3) NH. The fitted titration curves correspond to the parameters given in Table 2.

indication of a hydrogen bond to the carboxyl group of Asp(B9). As for a salt bridge, a possible partner could be the side chain of His(B10). However, the three-dimensional solution structure does not suggest any likely partners for the formation of a salt bridge with Asp(B9). Furthermore, a structure refinement calculation using X-PLOR (Brünger, 1992), in which a distance restraint (2 Å $\leq d \leq$ 3 Å) between the His(B10) N1H proton and one of the oxygen of the Asp(B9) carboxyl group was included in order to impose a close contact between the charged groups of these residues, gave rise to a severe distance violation between the β-protons of His(B10) and the γ-protons of Val(B12). Moreover, the C4H proton of His(B10) shows a titration shift at low pH with a pK_{app} that is close to the pK_a value of Glu(B13) (2.07 $\pm$ 0.17 and 2.20 $\pm$ 0.10) while significantly different from the pK_a value of 2.60 $\pm$ 0.05 observed for Asp(B9). Therefore, it seems likely that, in the native form of Asp(B9) insulin, His(B10) is involved in a salt bridge with Glu(B13) and *not* with Asp(B9) (*vide infra*). This is further supported by the observation of almost identical pK_a values for His(B10) in Asp(B9) insulin and biosynthetic human insulin (Bryant et al., 1993), (~7 and 6.7, respectively), which indicates that the negatively charged Asp(B9) does not interact with His(B10).

It is worth noting, however, that a salt bridge between Asp(B9) and His(B10) may exist in denatured insulin. Thus, model studies (data not shown) of the B8−B12 pentapeptide clearly indicated that a salt bridge between the Asp(B9) carboxyl group and the His(B10) imidazole ring is established in this peptide and, therefore, is likely to occur also in denatured Asp(B9) insulin.

A quantitative estimate of the stabilization of the native structure induced by the favorable interaction between the negatively charged Asp(B9) side chain and the α-helix dipole at neutral pH can be obtained from (Cantor & Schimmel, 1980)

$$pK' = pK_0 + \frac{\Delta G_c}{2.303RT} \quad (4)$$

Here pK' is the observed pK_a value, pK_0 is the pK_a value in the absence of the electrostatic interaction, and ΔG_c is the stabilization energy. A lower estimate of the stabilization energy can be obtained by using pK_{int} as pK_0, since Asp(B9) is not involved in any other favorable electrostatic interactions [the estimate is a lower limit, since an unfavorable interaction between Asp(B9) and Glu(B13) within the dimer is likely to occur, *vide infra*]. Therefore, the pK_a value of Asp(B9) corresponds to a stabilization energy of at least 1.9 kcal/mol in good agreement with previously suggested values (1.4−2.1 kcal/mol) for similar interactions (Serrano & Fersht, 1989; Šali et al., 1988; Nicholson et al., 1988). It should be mentioned that the interaction between Asp(B9) and the α-helix dipole thus observed is in contrast to previous model studies (Kaarsholm et al., 1993).

Specific Interresidue Interactions. The NMR titration experiments provide information about specific interresidue interactions, e.g., salt bridges and hydrogen bonds involving a carboxyl group, in two ways. First, they reveal the anomalous pK_a values of specific ionizable groups that take part in electrostatic interactions. Second, they can determine the two partners in the interresidue interaction since the chemical shifts of protons in both residues are affected by the same ionization. This holds not only for salt bridges (Turner et al., 1983; Abildgaard et al., 1992) but also for hydrogen bonds between amide protons and carboxyl groups, which can be identified by the observation of large downfield titration shifts of the amide protons with increasing pH, that are concomitant to the titration shifts of protons in the carboxyl group residue (Bundi & Wüthrich, 1979). Both types of interaction are observed in Asp(B9) insulin.

Formation of Salt Bridges. One of the most conspicuous results in Table 1 is the pK_a value of 2.20 $\pm$ 0.10 observed for Glu(B13). This value is 2.3 pK units lower than the corresponding pK_{int} value (4.5), which strongly suggests that the γ-carboxyl group of Glu(B13) is involved in a favorable electrostatic interaction. Most likely, this interaction is a salt bridge with the positively charged imidazole group of His(B10), since the side chains of Glu(B13) and His(B10) are close in space in the B-chain α-helix (Jørgensen et al., 1992). Further support for this salt bridge is the observation mentioned above that the C4H proton of His(B10) shows a titration shift with a pK_{app} value of 2.07 $\pm$ 0.17 (Figure 4 and Table 2), which is identical to the pK_a value of Glu(B13) within the experimental errors.

The salt bridge should also affect the pK_a value of the imidazole group of His(B10) and increase it by an amount comparable to the decrease of the pK_a value of Glu(B13) (Turner et al., 1983). It is therefore surprising that the observed pK_a value of His(B10) (~7) is close to the pK_{int} value of the imidazole ring. However, the pK_a value of His(B10) may also be affected by the B-chain α-helix since this residue, like Asp(B9), is positioned in the N-terminal end of the helix. Thus, Sancho et al. (1992) found pK_a values

Table 2: Ionization Constants and Titration Shifts for ^1H Resonances[a] of B9(Asp) Insulin at 295 K

residue	proton	$\Delta\delta^b$ (ppm)	pK_{app}
Val(A3)	NH	0.420	2.32 ± 0.09
	H^α	−0.111	2.61 ± 0.08
Gln(A5)	H^α	−0.061	2.48 ± 0.07
	H^β	−0.055	2.86 ± 0.14
	$H^{\gamma'}$	0.063	2.16 ± 0.31
Thr(A8)	H^α	−0.035	2.72 ± 0.07
	H^β	0.037	3.00 ± 0.18
Ser(A9)	NH	−0.216	2.66 ± 0.09
Ile(A10)	NH	−0.075	2.22 ± 0.19
	H^α	0.062	2.73 ± 0.20
	H^β	−0.034	2.89 ± 0.12
	H^γ	−0.047	2.32 ± 0.14
Leu(A16)	NH	−0.174	3.55 ± 0.06
Asn(A18)	H^β	−0.043	3.39 ± 0.12
	$H^{\delta'}$	−0.069	3.31 ± 0.11
Tyr(A19)	H^β	−0.039	2.87 ± 0.09
	$H^{\beta'}$	0.065	3.16 ± 0.09
His(B5)	NH	−0.089	3.75 ± 0.15
	C4H	0.044	2.31 ± 0.15
Leu(B6)	NH	0.064	1.95 ± 0.19
Gly(B8)	NH	0.110	2.51 ± 0.13
	H^α	0.065	2.17 ± 0.10
His(B10)	NH	−0.071	2.66 ± 0.10
	H^α	0.071	2.68 ± 0.15
	C4H	0.050	2.07 ± 0.17
Val(B12)	H^α	−0.101	2.41 ± 0.10
	H^β	−0.144	2.62 ± 0.04
Glu(B13)	NH	−0.158	2.69 ± 0.07
Ala(B14)	NH	−0.093	2.09 ± 0.09
	H^α	−0.071	3.31 ± 0.08
Leu(B15)	NH	−0.071	3.29 ± 0.13
	$H^{\beta'}$	0.073	2.01 ± 0.10
Tyr(B16)	NH	0.119	2.09 ± 0.07
	$H^{\beta'}$	0.059	2.67 ± 0.18
	H^δ	0.058	2.02 ± 0.13
Leu(B17)	NH	0.253	2.58 ± 0.08
	H^α	−0.052	2.76 ± 0.09
	H^β	−0.122	2.49 ± 0.06
	H^γ	0.109	2.18 ± 0.13
Val(B18)	NH	−0.104	3.26 ± 0.05
Gly(B20)	NH	0.095	3.21 ± 0.10
Glu(B21)	H^β	−0.046	3.07 ± 0.11
Arg(B22)	H^β	0.141	3.30 ± 0.20
	H^ϵ	0.402	3.24 ± 0.07
Phe(B24)	NH[c]	−0.112	3.90 ± 0.18
Pro(B28)	H^δ	−0.055	3.09 ± 0.14

[a] No intraresidual signals could be followed from the following residues: Gly(A1), Ile(A2), Cys(A6), Cys(A7), Cys(A11), Cys(A20), Cys(B7), Gly(B8), Leu(B11), Cys(B19), Phe(B24), Phe(B25), and Tyr(B26). [b] $\Delta\delta = \delta_2 - \delta_1$. [c] Chemical shift measured from a sequential NOE to B23 NH.

of 5.82 and 5.68 for the histidines placed at the N-terminal ends of the two helices in barnase. These results suggest that the pK_a value of His(B10) in the absence of interactions other than those with the α-helix dipole would be ≤6 rather than 6.8. Moreover, other structural changes that take place in the monomer−monomer interface with increasing pH (*vide infra*) may also influence the pK_a of His(B10). Therefore, the pK_a value of ~7 observed for His(B10) does not disagree qualitatively with the formation of the salt bridge between the side chains of Glu (B13) and His(B10).

The salt bridge between His(B10) and Glu(B13) is interesting since it is an example of an i, $i + 3$ salt bridge which, presumably, is less likely to occur in an α-helix than the i, $i + 4$ salt bridge (Thornton, 1992). It is also interesting to notice that although the salt bridge undoubtedly stabilizes the α-helix it is not essential for the formation of the helix. This is clearly demonstrated by the fact that the helix is well-

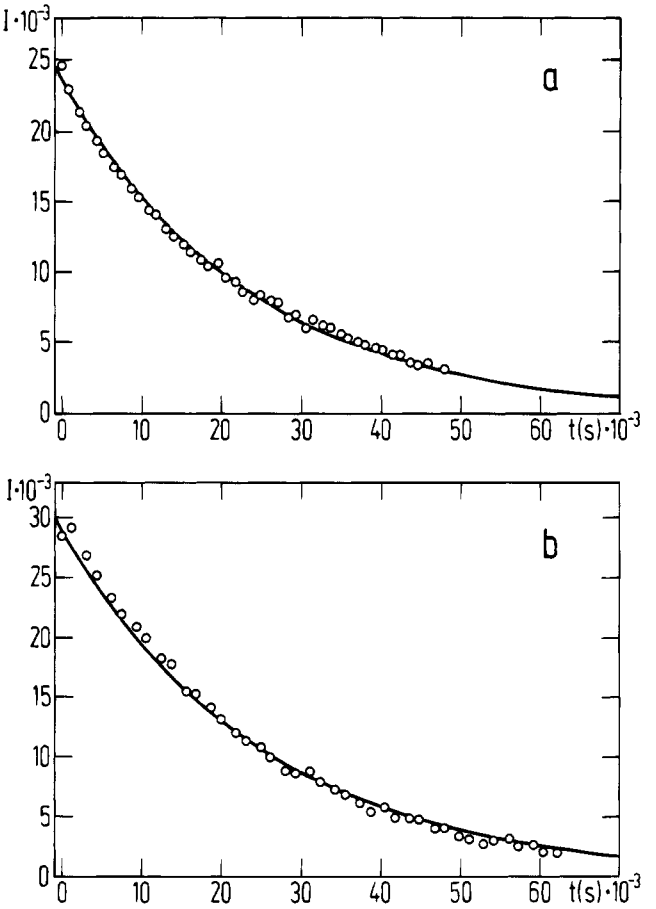

FIGURE 5: Fits of the parameters in eq 3 to the intensities of the Phe(B24) NH signal as function of time at (a) pH 1.92 and (b) pH 3.03. The obtained exchange rates for Phe(B24) NH are (43.3 ± 0.5) × 10^{-6} s^{-1} and (40.1 ± 0.6) × 10^{-6} s^{-1} at pH 1.92 and 3.03, respectively.

established at pH 1.9 (Jørgensen et al., 1992), that is, at a pH value where the salt bridge does not exist. This observation is in agreement with the general conclusion that the contribution from salt bridges to the stability of proteins is only minor (Serrano et al., 1992).

Also the formation of a salt bridge between the carboxyl group of Asn(A21) and the guanidinium group of Arg(B22) is evidenced by the titration data. In the structure of Asp(B9) insulin at pH 1.9 (Jørgensen et al., 1992) this salt bridge is not established, although the two groups are close in space. However, the low pK_a value (3.17 ± 0.04, Table 1) found here for the carboxyl group of Asn(A21) shows that the deprotonated form of Asn(A21) is involved in a favorable electrostatic interaction. This together with an identical pK_{app} value (3.24 ± 0.07, Figure 4 and Table 2) observed for the ϵ-proton of Arg(B22) strongly indicates the formation of the salt bridge. A similar salt bridge was found in the 2Zn insulin crystal structure (Blundell et al., 1972).

Further evidence of the formation of the salt bridge between Asn(A21) and Arg(B22) is given by the titration shifts of a number of protons of the adjacent residues [Asn(A18) $H^{\delta'}$, Tyr(A19) $H^{\beta'}$, Val(B18) NH, Gly(B20) NH, Glu(B21) H^β]. These shifts all correspond to pK_{app} values that are practically identical to the pK_a value of Asn(A21) (Table 2). These shifts undoubtedly reflect the structural change that accompanies the formation of the salt bridge between Asn(A21) and Arg(B22).

The low pK_a value (2.62 ± 0.06) of the Glu(A4) carboxyl group is difficult to rationalize on the basis of the experimental results. However, this pK_a value could be a consequence of the formation of a salt bridge with the amino group of Gly(A1), leading to a more regular A_1 α-helix at higher pH. This suggestion is supported by the titration shifts of Val(A3) H^α, Gln(A5) H^α, Thr(A8) H^α, and Ser(A9) NH, all of which correspond to pK_{app} values (Table 2) close to the pK_a value of Glu(A4). Also in this case, a corresponding salt bridge is observed in the 2Zn insulin structure (Baker et al., 1988).

Evidence for Hydrogen Bond between Val(A3) NH and Thr(B30) COOH. The slow exchange of the amide proton of Val(A3) could not be attributed, unambiguously, to a specific hydrogen bond in the solution structure at pH 1.9 (Jørgensen et al., 1992), although restrained molecular dynamics calculations indicated that it could be involved in a hydrogen bond to the carbonyl oxygen of Gly(A1). Here, the results of the titration experiments provide new information about the hydrogen bonding of Val(A3) NH. The most conspicuous result in this context is the observation of a pK_a value of the Thr(B30) carboxyl group that is low and practically identical to the pK_{app} value of the Val(A3) NH proton. This together with the fact that the N-terminus of the A-chain makes close contact with the C-terminus of the A-chain (Baker et al., 1988; Jørgensen et al., 1992) immediately suggest that the amide proton of Val(A3) is involved in a hydrogen bond with the carboxyl group of Thr(B30). A similar hydrogen bond was identified in BPTI (Bundi & Wüthrich, 1979) between the side-chain carboxyl group and the amide proton of Glu49. In both studies, a substantial decrease of the pK_a value of the carboxyl group was observed together with a downfield titration shift of about 0.4 ppm of the involved amide proton.

The fact that a *downfield* titration shift is observed for the A3 NH (Figure 4 and Table 2) shows that the hydrogen bond is preserved in the investigated pH range, since a breaking of the bond would give rise to an upfield titration shift. Hence, the dramatic change in the shielding of the amide proton is a consequence of the titration of the Thr(B30) carboxyl group.

Further support of the hydrogen bond between the Val(A3) amide proton and the carboxyl group of Thr(B30) was given by a structure refinement calculation using X-PLOR (Brünger, 1992), which includes the distance restraints imposed by the hydrogen bond. First, the calculation showed that there is no inconsistency between the hydrogen bond and the other structural restraints. Moreover, the refined structure shows a close contact between Glu(A4) and Thr(B30). Immediately this result prompted a reexamination of the NOESY spectrum recorded at pH 1.9, which revealed a few weak NOEs between these residues (Figure 6) that have not been observed previously. Therefore, taken together the experimental evidence presented here suggest that a hydrogen bond is established between the Val(A3) amide hydrogen and the Thr(B30) carboxyl group.

Characterization of pH-Induced Structural Changes in Monomer−Monomer Interface. The structure of the insulin dimer is well described both in the crystal phase (Blundell et al., 1972; Baker et al., 1988) and in solution (Jørgensen et al., 1992). In both phases, the principal interactions involve B8, B9, B12, B16, and B23−B28. Since the monomer is the biologically active form of insulin, much

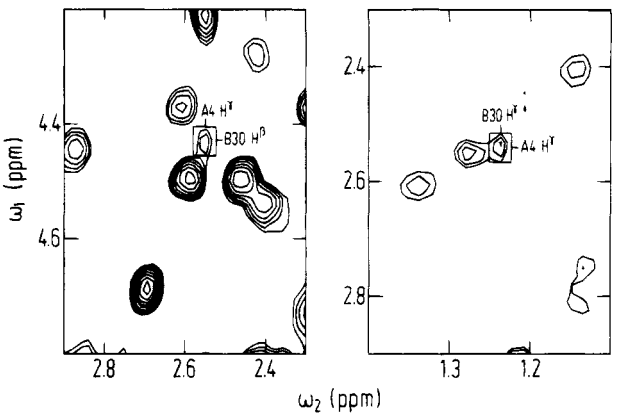

FIGURE 6: Region of a NOESY spectrum of Asp(B9) insulin in H_2O (5 mM, pH 1.90, 295 K) showing correlations between Thr(B30) and Glu(A4). The NOESY spectrum is the same one as shown by Figure 3 of Kristensen et al. (1991).

effort has been made to design a biologically active mutant that stays monomeric in solution at pharmaceutical concentrations. To that end, a series of insulin analogues was suggested (Brange et al., 1988) in which charge repulsion was introduced into the monomer−monomer interface in order to promote monomerization. The Asp(B9) mutant studied here is one of the most successful analogues in that series. Thus, at pH 7.5 and a concentration of 1 mM, the average molecular weight of the Asp(B9) mutant was found to be only about 10% higher than the molecular weight of the monomer. The success of the mutant to monomerize was ascribed to the fact that the dimer packing brings the two Asp(B9) residues and the two Glu(B13) residues within 4 Å. At neutral pH, this results in a electrostatic repulsion between the four negatively charged side-chain carboxyl groups, which is large enough to prevent dimerization.

In view of this, the results of the titration experiments here are intriguing. Primarily, the data indicate that structural changes do take place in the monomer−monomer interface when the side-chain carboxyl groups of Glu(B13) and Asp(B9) are ionized. Thus, the observed titration shifts of the amide protons of Ala(B14) and Tyr(B19) with pK_{app} values close to the pK_a value of Glu(B13) (Table 2) show that these protons are affected by the ionization of Glu(B13). Similarly, the observed titration shifts of the amide protons of Gly(B8), Asp(B9), His(B10), Glu(B13), and Leu(B17) with pK_{app} values close to the pK_a value of Asp(B9) (Table 2) show that these protons are affected by the ionization of Asp(B9). Therefore, the ionizations of Glu(B13) and Asp(B9) do give rise to structural changes in the monomer−monomer interface B8−B16.

However, in spite of these structural changes, the dimer remains intact in the entire pH range investigated here (1.73−3.71); that is, the Asp(B9) mutant is still a dimer at pH values where the side-chain carboxyl groups of Glu(B13) and Asp(B9) are both ionized. This surprising result is revealed by a series of observations.

First, some of the intermolecular NOEs that characterize the dimer at pH 1.9 (Jørgensen et al., 1992) are also observed at pH 3.03. In particular, the intermolecular NOEs between Gly(B23) H^α and Tyr(B26) H^δ and between Gly(B23) H^α and Tyr(B26) H^α are preserved at pH 3.03. Also at the monomer−monomer interface B8−B16, weak NOEs corresponding to the interaction between Tyr(B16) H^β and

Tyr(B26) H^{δ} and between Gly(B8) H^{α} and Tyr(B16) H^{ϵ} could be detected.

Second, the chemical shifts of the amide protons of Phe(B24) and Tyr(B26) are practically independent of pH in the pH range 1.73−3.71, as shown in Figure 3. Since these amide protons are involved in the four intermolecular hydrogen bonds of the antiparallel β-sheet that characterizes the dimer (Blundell et al., 1972; Jørgensen et al., 1992), the transition to the monomer where these hydrogen bonds are absent would have resulted in a substantial change in the chemical shift of the two amide protons.

Third, the exchange rate of the amide proton of Phe(B24) is almost identical at pH 1.92 and pH 3.03, respectively, as shown in Figure 5. Again, a monomerization would have resulted in a dramatic increase of this exchange rate because of the absence of the intermonomer hydrogen bonds between the amide protons of the two Phe(B24) residues and the carboxyl oxygens of the two Tyr(B26) residues. A corresponding evaluation of the exchange rate of the Tyr(B26) amide proton could not be made because of severe spectral overlap in the 1D spectra.

Immediately, this dimerization of the Asp(B9) analogue at pH values where the side-chain carboxyl groups of Asp(B9) and Glu(B13) are both ionized seems to be in conflict with the monomerization found by Brange et al. (1988). However, it should be noted that the latter result was obtained at pH 7.5, that is, at a pH where the imidazole rings of His(B5) and His(B10) are uncharged, while the result here is obtained at pH values where the imidazole rings of the histidines are positively charged. Therefore, since His(B10) is located in the monomer−monomer interface, the neutralization of the charge of its imidazole ring at the pH applied by Brange et al. increases the total negative charge in the interface and, thus, increases the repulsion as compared to the repulsion at pH values below the $pK_a \sim 7$ of His(B10). As indicated by the observations of Brange et al. (1988), the resulting repulsion is sufficiently large to enforce the monomerization.

CONCLUSIONS

The present study demonstrates that detailed and versatile structural information about proteins can be obtained from multi-dimensional NMR titration studies when the sequential assignment of the ^1H NMR spectrum and the three-dimensional solution structure of a protein are available. Specifically, for the dimeric Asp(B9) mutant of human insulin, the study reveals the presence of a series of electrostatic interactions and a hydrogen bond through their pH dependence. Most surprisingly, it reveals that the mutants remains dimeric above the pH value at which both of the side-chain carboxyl groups of Glu(B13) and Asp(B9) are ionized.

ACKNOWLEDGMENT

We thank Drs. Georg Ole Sørensen and Henrik Gesmar for computational assistance, Dr. Søren M. Kristensen for recording the 2D NOESY spectra, and Dr. Per Balschmidt, Novo Nordisk, for providing the Asp(B9) mutant of human insulin.

REFERENCES

Abildgaard, F., Gesmar, H., & Led, J. J. (1988) *J. Magn. Reson. 79*, 78−89.

Abildgaard, F., Jørgensen, A. M. M., Led, J. J., Christensen, T., Jensen, E. B., Junker, F., & Dalbøge, H. (1992) *Biochemistry 31*, 8587−8596.

Baker, E. N., Blundell, T. L., Cutfield, J. F., Cutfield, S. M., Dodson, E. J., Dodson, G. G., Hodgkin, D. M. C., Hubbard, R. E., Isaacs, N. W., Reynolds, C. D., Sakabe, K., Sakabe, N., & Vijayan, N. M. (1988) *Philos. Trans. R. Soc. London, B 319*, 369−456.

Blundell, T. L., Dodson, G. G., Hodgkin, D. M. C., & Mercola, D. A. (1972) *Adv. Protein Chem. 26*, 279−402.

Bodenhausen, G., Vold, R. L., & Vold, R. R. (1980) *J. Magn. Reson. 37*, 93−106.

Brange, J., Ribel, U., Hansen, J. F., Dobson, G., Hansen, M. T., Havelund, S., Melberg, S. G., Norris, F., Norris, K., Snel, L., Sørensen, A. R., & Voigt, H. O. (1988) *Nature 333*, 679−682.

Brünger, A. T. (1992) X-PLOR version 3.1. A system for X-Ray crystallography and NMR. *X-PLOR Manual*, Yale University, CT.

Bryant, C., Spencer, D. B., Miller, A., Bakaysa, D. L., McCune, K. S., Maple, S. R., Pekar, A. H., & Brems, D. N. (1993) *Biochemistry 32*, 8075−8082.

Bundi, A., & Wüthrich, K. (1979) *Biopolymers 18*, 299−311.

Cantor, C. R., & Schimmel, P. R. (1980) *Biophysical Chemistry*, pp 42−51, Freeman, San Francisco.

Drobny, G., Pines, A., Sinton, S., Weitekamp, D. P., & Wemmer, D. (1979) *Faraday Symp. Chem. Soc. 13*, 49−55.

Hoult, D. I. (1976) *J. Magn. Reson. 21*, 337−347.

Jeener, J., Meier, B. H., Bachmann, P., & Ernst, R. R. (1979) *J. Chem. Phys. 71*, 4546−4553.

Jørgensen, A. M. M., Kristensen, S. M., Led, J. J., & Balschmidt, P. (1992) *J. Mol. Biol. 227*, 1146−1163.

Kaarsholm, N. C., Norris, K., Jørgensen, R. J., Mikkelsen, J., Ludvigsen, S., Olsen, O. H., Sørensen, A. R., & Havelund, S. (1993) *Biochemistry 32*, 10773−10778.

Kohda, D., Sawada, T., & Inagaki, F. (1991) *Biochemistry 30*, 4896−4900.

Kristensen, S. M., Jørgensen, A. M. M., Led, J. J., Balschmidt, P., & Hansen, F. B. (1991) *J. Mol. Biol. 218*, 221−231.

Macura, S., Huang, Y., Suter, D., & Ernst, R. R. (1981) *J. Magn. Reson. 43*, 259−281.

Marion, D., & Wüthrich, K. (1983) *Biochem. Biophys. Res. Commun. 1133*, 967−974.

Marion, D., Ikura, M., & Bax, A. (1989) *J. Magn. Reson. 84*, 425−430.

Nicholson, H., Becktel, W. J., & Matthews, B. W. (1988) *Nature 336*, 651−656.

Redfield, A. G., & Kunz, S. D. (1975) *J. Magn. Reson. 19*, 250−254.

Šali, D., Bycroft, M., & Fersht, A. R. (1988) *Nature 335*, 740−743.

Sancho, J., Serrano, L., & Fersht, A. R. (1992) *Biochemistry 31*, 2253−2258.

Serrano, L., & Fersht, A. R. (1989) *Nature 342*, 296−299.

Serrano, L., Kellis, J. T., Jr., Cann, P., Matouschek, A., & Fersht, A. R. (1992) *J. Mol. Biol. 224*, 783−804.

States, D. J., & Karplus, M. (1987) *J. Mol. Biol. 197*, 122−130.

Thornton, J. M. (1992) in *Protein Folding* (Creighton, T. E., Ed.) pp 71−73, W. H. Freeman and Company, New York.

Turner, C., Cary, P. D., Grego, B., Hearn, M. T. W., & Chapman, G. E. (1983) *Biochem. J. 213*, 107−113.

Zuiderweg, E. R. P., Hallenga, K., & Olejniczak, E. T. (1986) *J. Magn. Reson. 70*, 336−343.